

Evolution of Very Massive Population III Stars with Mass Accretion from Pre-Main Sequence to Collapse

Takuya Ohkubo^{1,2}, Ken'ichi Nomoto^{2,1}, Hideyuki Umeda¹,
Naoki Yoshida^{2,3}, and Sachiko Tsuruta⁴

ABSTRACT

We calculate the evolution of zero-metallicity Population III (Pop III) stars whose mass grows from the initial mass of $\sim 1M_{\odot}$ by accreting the surrounding gases. Our calculations cover a whole evolutionary stages from the pre-main sequence, via various nuclear burning stages, through the final core collapse or pair-creation instability phases. We adopt the following stellar mass-dependent accretion rates which are derived from cosmological simulations of early structure formation based on the low mass dark matter halos at redshifts $z \sim 20$: (1) the accretion rates for the first generation (Pop III.1) stars and (2) the rates for zero-metallicity but the second generation (Pop III.2) stars which are affected by radiation from the Pop III.1 stars. For comparison, we also study the evolution with the mass-dependent accretion rates which are affected by radiative feedback. We show that the final mass of Pop III.1 stars can be as large as $\sim 1000M_{\odot}$, beyond the mass range ($140 - 300M_{\odot}$) for the pair-instability supernovae. Such massive stars undergo core-collapse to form intermediate-mass black holes, which may be the seeds for merger trees to supermassive black holes. On the other hand, Pop III.2 stars become less massive ($\lesssim 40 - 60M_{\odot}$), being in the mass range of ordinary iron core-collapse stars. Such stars explode and eject heavy elements to contribute to chemical enrichment of the early universe as observed in the abundance patterns of extremely metal-poor stars in the Galactic halo.

Subject headings: accretion, accretion disks – nuclear reactions, nucleosynthesis, abundances – stars: abundances – stars: evolution – stars: formation – supernovae: general

1. INTRODUCTION

Just after the Big Bang, a cosmic primordial gas consists mostly of H, He and a small amount of light elements (Li, Be, B, etc). The first heavier elements, such as C, O, Ne, Mg, Si and Fe, must be synthesized during the evolution of the

first (metal-free = Population III = Pop III) stars early in the history of the universe. It is generally thought that massive Pop III stars distribute synthesized heavy elements by supernova explosions (e.g., Nomoto et al. 2006).

If Pop III stars are sufficiently massive, they could also form intermediate mass black holes (IMBHs) ($\sim 5 \times 10^2 - 5 M_{\odot}$). The formation of IMBHs would have important implications. Stellar mass black holes ($\sim 10M_{\odot}$) are formed as the central compact remnants of ordinary massive ($25 - 140M_{\odot}$) stars at the end of their evolution. Supermassive black holes (SMBHs) ($\sim 10^5 - 10^9 M_{\odot}$) are now known to exist in the center of almost all galaxies (e.g., Kormendy & Richstone 1995; Bender 2005), but their formation processes are largely unknown. Recently, the role of IMBHs caught much attention in the context of the for-

¹Department of Astronomy, School of Science, University of Tokyo, 7-3-1 Hongo, Bunkyo-ku, Tokyo 113-0033, Japan; ohkubo@astron.s.u-tokyo.ac.jp, umeda@astron.s.u-tokyo.ac.jp

²Institute for the Physics and Mathematics of the Universe (IPMU), University of Tokyo, 5-1-5 Kashiwanoha, Kashiwa, Chiba 277-8568, Japan; nomoto@astron.s.u-tokyo.ac.jp, naoki.yoshida@ipmu.jp

³Department of Physics, Nagoya University, Furocho, Chikusa-ku, Nagoya 464-8602, Japan

⁴Department of Physics, Montana State University, Bozeman, MT 59717-3840; uphst@gemini.msu.montana.edu

mation of SMBHs. One of the viable scenarios for SMBH formation is a merger tree model in which seed black holes of a few $\times 10^2 M_\odot$ formed early (e.g., at $z \sim 20$) are assumed to have merged and grown to become SMBHs (e.g., Madau and Rees 2001; Volonteri et al. 2003). In this model, the small seed blackholes generally go through IMBH stages at some intermediate epochs, e.g., between $z \sim 20$ and 0.

For both chemical enrichment and the formation of IMBHs in the early universe, the massive Pop III stars may play important roles. In order to clarify the fate of Pop III stars which depends sensitively on the stellar mass, M , we study the evolution of mass accreting Pop III stars. In the present paper, we generally call stars with mass $M > 100 M_\odot$ very massive stars (VMSs). Among VMSs, we refer to stars with $M > 300 M_\odot$ as core-collapse very massive stars (CVMSs) (Ohkubo et al. 2006).

The standard cosmological model based on dark energy and cold dark matter (CDM), the so-called Λ CDM model, posits that structure forms hierarchically from smaller mass objects (a bottom-up scenario; Davis et al. 1985; Ostriker & Steinhardt 2003; Kirshner 2003). Small density fluctuations in the early universe seed nonlinear growth of structure via gravitational instability. According to this model, smaller, stellar size objects formed first and then larger structures such as galaxies are assembled by merging of these smaller units. The first generation stars are predicted to be formed when the age of the universe was less than a few hundred million years (Couchman & Rees 1986; Tegmark et al. 1997; Yoshida et al. 2003), whereas, observationally, the WMAP data suggests that it is $z \sim 10$ (Sanchez et al. 2006; Spergel et al. 2007).

In the early universe, dark matter plays an important role for the formation of the first generation stars. Dark matter (DM) gathers due to gravity and forms minihalos with typical mass of $\sim 10^6 M_\odot$ (Haiman et al. 1996; Tegmark et al. 1997; Fuller & Couchman 2000). After the formation of minihalos, the baryon gas gravitationally collapses to form a star. Since the primordial gas contains no heavy elements, molecular hydrogen is the only efficient coolant indispensable for star formation (Peebles & Dicke. 1968; Matsuda et al. 1969; Palla et al. 1983).

Theoretical studies on star formation suggest that the initial mass function (IMF) of Pop III first stars may be different from the present one, possibly dominated by very massive stars (e.g., Omukai & Nishi 1998; Nakamura & Umemura 1999; Abel et al. 2002; Bromm et al. 1999; Omukai & Palla 2003). A number of numerical simulations of the formation of the first stars have been carried out. They are, either one-dimension calculations (Haiman et al. 1996; Nakamura & Umemura 2002; Ahn & Shapiro 2007) or three dimensional simulations (Abel et al. 2000, 2002; Bromm et al. 1999; Bromm & Larson 2003; Fuller & Couchman 2000; Yoshida et al. 2006; O’Shea & Norman 2006a,b; Gao et al. 2007). These studies generally suggest that the typical mass of a primordial gas cloud is $\sim 10^3 - 10^5 M_\odot$. The latest detailed calculations have shown that a protostellar core of as small as $M \sim 10^{-2} M_\odot$ is formed at the center of a primordial gas cloud (Yoshida et al. 2008). After such a small proto-stellar core is formed, the gas surrounding it accretes on the protostar and the stellar mass increases through the pre-main sequence stage.

A crucial parameter is the mass accretion rate, which determines the typical mass of Pop III stars (e.g. Tan & McKee 2004). Cosmological simulations (e.g. Abel et al. 2002; Bromm & Loeb 2004; Yoshida et al. 2006; Gao et al. 2007) have shown that the accretion rate is as high as $\dot{M} \sim 10^{-2} M_\odot \text{ yr}^{-1}$ when the core mass is small ($M \lesssim 10 M_\odot$) and it decreases with increasing mass. These studies have suggested that first stars might be more massive than $100 M_\odot$, in the zero-metallicity environment. Omukai & Palla (2003) calculated protostar evolution with constant accretion rates. They treated the accretion rate as a free parameter and set it to be of the order of $\dot{M} \sim 10^{-2} M_\odot \text{ yr}^{-1}$ and obtained that the final mass could exceed $100 M_\odot$. However, they also found that, if $\dot{M} > 4 \times 10^{-3} M_\odot \text{ yr}^{-1}$, the stellar radius rapidly expands to prevent further growth. Thus the final fate could not be predicted. If mass accretion continues through its lifetime (\sim a few $\times 10^6$ years), i.e., if mass accretion is not impeded by feedback from the star itself, the final mass may reach several times $10^2 M_\odot$ or more.

Stars formed in the way described above (which are called ‘Pop III.1’ stars; McKee & Tan 2008) radiate a large amount of UV photons and build

up HII regions with a few kiloparsec diameter (Yoshida et al. 2007). This environment promotes the formation of HD molecules, which can cool the gas down to as low as 40 – 50K. In a gas cloud at such low temperatures, typical stellar mass formed is $\sim 40M_{\odot}$, smaller than Pop III.1 stars. Stars formed in such environment are called ‘Pop III.2’ stars (McKee & Tan 2008; Johnson et al. 2008).

The possibility of the formation of VMSs as Pop III.1 stars has renewed the interest in the final fate of such VMSs. Previous studies, which did not take into account mass accretion, have shown that the final fate of the VMSs is sensitive to the stellar mass M (e.g., Barkat et al. 1967; Rakavy & Shaviv 1968; Ober et al. 1983; Bond et al. 1984; Arnett 1996). If $M > 300M_{\odot}$, the stars undergo core-collapse to form IMBHs, which we call CVMS. If $M \simeq 140 - 300M_{\odot}$, the stars undergo pair instability supernovae (PISNe) and disrupt completely, ejecting a large amount of heavy elements. Thus PISNe have been suggested to be the main source of chemical enrichment in the early universe. However, recent detailed comparisons between the observations of extremely metal poor (EMP) stars (Cayrel et al. 2004) and the nucleosynthesis yields of PISN models (Umeda & Nomoto 2002; Heger & Woosley 2002) have shown that the PISN yields are hard to reproduce the abundance patterns of EMP stars (Cayrel et al. 2004).

It is interesting to examine theoretically under what conditions the Pop III stars end their lives as PISNe. The related question of whether CVMSs ($M \sim 300 - 10^5 M_{\odot}$) could actually form is of great importance, for instance, to understand the origin of IMBHs. For this purpose, in this paper we adopt the realistic mass accretion rate obtained by Yoshida et al. (2006), which follows the evolution of dense gas clumps formed at the centers of rather low mass ($\sim 10^{5-6} M_{\odot}$) dark matter halos at redshifts $z \simeq 20$.

In the present paper, we calculate stellar evolution of Pop III stars growing by accretion and investigate the final fate of such stars. So far all previous calculations of protostar evolution ended at the onset of hydrogen burning, at the start of the main sequence, and hence they do not answer the question of how such massive Pop III objects evolve after they start hydrogen burning and what the final stellar mass can be. Therefore, the ma-

ior purpose of the current studies is not only to follow the pre-main sequence evolution studied by Omukai & Palla (2003) and Yoshida et al. (2006), but also to continue further stellar evolution by adopting the mass accretion rate obtained by the cosmological simulation (Yoshida et al. 2006). We calculate whole nuclear burning stages, until the point where the star ends its life with core collapse and/or explosion.

Following the introduction in this section, our models are described in Section 2 and our results are presented in Section 3. In the last two sections, 4 and 5, we give discussion, summary and concluding remarks.

2. MODELS IN PRESENT STUDIES

In Ohkubo et al. (2006), we calculated evolution, nucleosynthesis, explosion and collapse of Pop III CVMSs starting from the main-sequence in the absence of mass accretion. More realistically Pop III stars are formed along with cosmological structure formation, and the mass increases by accretion and the final mass may be in the range of VMS ($M > 100M_{\odot}$). In the present study, we calculate the evolution of Pop III stars with mass accretion, starting from the pre main-sequence phase with small mass comparable to the solar mass, until core collapse or pair instability explosion. In this subsection we summarize our models and assumptions at the initial and each subsequent stage.

To calculate presupernova evolution through the early hydrodynamical phase, we adopt the Henyey-type hydrodynamical stellar evolution code (Nomoto 1982; Nomoto & Hashimoto 1988; Umeda et al. 1999; Umeda & Nomoto 2002, 2005). The mass accretion is calculated with the method of Neo et al. (1976) and Nomoto (1982). We adopt the nuclear reaction network developed by Hix & Thielemann (1996) for calculating nucleosynthesis and energy generation at each stage of the evolution. We include 51 isotopes up to Si until He burning ends, and 240 up to Ge afterwards.

We start with a $1.5M_{\odot}$ pre main-sequence star, a typical mass size in the low-mass star ranges. We investigate how this low mass stellar core grows up to a massive one with gas accretion. The starting mass of $1.5M_{\odot}$ is larger than the initial mass set by Omukai & Palla (2003), $0.01M_{\odot}$, by more than

two orders of magnitude. However, the time it takes for the star to increase its mass from $0.01M_{\odot}$ to $1M_{\odot}$ is $\sim 10^2$ yr. This is negligible compared with the overall lifetime of a star. Physically, convection over the whole star occurs in the contracting phase. So the starting point little affects the later evolution, and as one can see later, we can qualitatively reproduce the protostellar evolution shown in Omukai & Palla (2003). Since we consider Pop III stars the chemical composition chosen are $X(\text{H}) = 0.753$, $X(\text{D}) = 2 \times 10^{-5}$, $X(^3\text{He}) = 2 \times 10^{-5}$, $X(^4\text{He}) = 0.247$, and $X(^7\text{Li}) = 2 \times 10^{-10}$.

The most important parameter in this work is the mass accretion rate, \dot{M} . We change this value and investigate how the star evolves and how large the final mass is. We choose the mass accretion rate calculated with three dimensional cosmological simulations by Yoshida et al. (2006) and Yoshida et al. (2007). These authors calculated cosmological structure formation in a Λ CDM universe and evaluated the accretion rate for Pop III stars. We approximate \dot{M} from their results as a function of stellar mass M :

$$\dot{M} = \frac{dM_Y}{dt} = \begin{cases} 0.0450 \times M^{-2/3} M_{\odot}\text{yr}^{-1} & M < 300M_{\odot} \\ 16.3 \times M^{-1.7} M_{\odot}\text{yr}^{-1} & M \geq 300M_{\odot} \end{cases} \quad (1)$$

for Pop III.1 stars (by Yoshida et al. 2006), and

$$\dot{M} = \frac{dM_{YII}}{dt} = \begin{cases} 0.0250 \times M^{-0.4} M_{\odot}\text{yr}^{-1} & M \leq 10M_{\odot} \\ 0.10 \times M^{-1.0} M_{\odot}\text{yr}^{-1} & 10M_{\odot} < M < 40M_{\odot} \\ 0 & M \geq 40M_{\odot} \end{cases} \quad (2)$$

for Pop III.2 stars (by Yoshida et al. 2007). These accretion rates are shown in Figure 1. We mark the former accretion rate with a subscript ‘Y’, as dM_Y/dt (Equation 1). We also adopt models with accretion rates smaller than dM_Y/dt by a factor of 2, 3, 10, and 20. We call these models ‘Y-series’. The latter accretion rate (Equation 2) is labeled ‘YII’, as dM_{YII}/dt (we distinguish this model from ‘Y-series’). For this model, the accretion rate is much lower than dM_Y/dt , because the gas temperature can become low in the fossil HII regions around the first generation stars (Yoshida et al. 2007). In Table 1, the models we calculate are

summarized.

Protostellar feedback effects may considerably affect the mass accretion, hence the protostar’s growth. Kudritzki (2000) argued that the effect of radiation pressure is probably negligible for a Pop III star since it has no metal. We discuss more recent studies later in this section. McKee & Tan (2008) showed that radiative feedback, if significant, can stop mass accretion when the stellar mass exceeds $\sim 100M_{\odot}$. If so, Pop III stars around this mass range may exist.

We also adopt accretion rates by McKee & Tan (2008), who take interruption by feedback into consideration. In their calculation, the accretion rate is very high in the proto-star phase, but when they reach the main-sequence, the accretion rate drops drastically owing to evaporation of the accretion disk by ionizing photons. During the main-sequence, accretion completely stops when outflow and inflow become the same. They parametrized a measure of entropy of the accreting gas, and subsequent accretion rate varies by more than one order of magnitude by changing this parameter. In this paper, we adopt typical three accretion rates. We approximate \dot{M} from figure 9 in McKee & Tan (2008) as follows

$$\dot{M} = \frac{dM_{M1}}{dt} = \begin{cases} 0.125 \times M^{-0.44} M_{\odot}\text{yr}^{-1} & M \leq 81M_{\odot} \\ 178 \times M^{-2.1} M_{\odot}\text{yr}^{-1} & 81M_{\odot} < M < 321M_{\odot} \\ 0 & M \geq 321M_{\odot}, \end{cases} \quad (3)$$

$$\dot{M} = \frac{dM_{M2}}{dt} = \begin{cases} 0.0250 \times M^{-0.44} M_{\odot}\text{yr}^{-1} & M \leq 41M_{\odot} \\ 20.0 \times M^{-2.3} M_{\odot}\text{yr}^{-1} & 41M_{\odot} < M < 135M_{\odot} \\ 0 & M \geq 135M_{\odot}, \end{cases} \quad (4)$$

and

$$\dot{M} = \frac{dM_{M3}}{dt} = \begin{cases} 0.005 \times M^{-0.44} M_{\odot}\text{yr}^{-1} & M \leq 25M_{\odot} \\ 32 \times M^{-3.2} M_{\odot}\text{yr}^{-1} & 25M_{\odot} < M < 57M_{\odot} \\ 0 & M \geq 57M_{\odot}. \end{cases} \quad (5)$$

These are marked ‘M’, as dM_{Mi}/dt ($i = 1, 2, 3$). We call these models ‘M-series’ and we summarize them in Table 1. These accretion rates are shown in Figure 2.

A Pop III star has initially no metal content by definition, and thus the line-driven stellar wind is thought to be negligible (Kudritzki 2000). There are some mechanisms which lead to mass loss - pulsational instability by the ϵ mechanism. However, the time scale of amplification of such oscillations is longer than the nuclear burning time scale of the main sequence ($\sim 10^6$ years) for Pop III stars, and so a star may evolve without losing a significant fraction of its initial mass (Ibrahim et al. 1981; Baraffe et al. 2001; Nomoto et al. 2003). On the other hand, there are other authors who carried out stellar evolution with mass loss even for very low-metallicity massive stars. Meynet et al. (2006) and Hirschi (2007) calculated pre-supernova evolution of very-metal poor stars (down to $Z = 5 \times 10^{-7} Z_{\odot}$) with rotation and found that such metal-poor stars can lose mass because the CNO elements which are synthesized in the deep interior are transported to the surface due to the rotational mixing. As long as mass accretion continues a typical accretion rate ($\gtrsim 10^{-3} M_{\odot}\text{yr}^{-1}$) is much higher than the mass loss rate, and hence in the present study mass loss is not considered.

3. RESULTS

3.1. Pre Main-Sequence Phase

Our evolutionary calculation starts from $M = 1.5M_{\odot}$. Figure 3 shows the evolutionary change in the stellar radius R as M increases for each model. It shows a few distinct evolutionary phases: pre main-sequence phase, main-sequence phase, and later phase. Each phase is partitioned with marks.

Because of the gravitational energy release and associated heating, the stellar radius quickly increases to as large as $R \sim 10^2 R_{\odot}$. At this point,

$\dot{M} \sim 10^{-2} M_{\odot}\text{yr}^{-1}$. After this rapid expansion, the star settles into the stage where the radius increases only gradually while adjusting to the mass accretion rate (see also Figure 3 in Neo et al. 1976). At this stage the stellar radius is given approximately by the stellar mass and mass accretion rate as:

$$R \propto M^{0.27} \dot{M}^{0.41}, \quad (6)$$

which is similar to the results by Stahler et al. (1986) and Omukai & Palla (2003). In the subsequent evolution, our models exhibit the similar trend to those shown in Omukai & Palla (2003; Fig.1) and Yoshida et al. (2006; Fig.13).

We started our calculations with mass accretion at $M = 1.5M_{\odot}$. In more realistic calculations Omukai & Palla (2003) and Yoshida et al. (2006) started their simulation of proto-stellar evolution with mass accretion with the very first core mass of $M \sim 10^{-3} M_{\odot}$, although their calculation ends at the end of the proto-star phase. The time it takes for the star to grow from $10^{-3} M_{\odot}$ to $1.5M_{\odot}$ is negligible compared with the lifetime of later phases, and this initial stage does not affect how massive the star can grow.

After the proto-star phase, the evolution depends on the timescales of accretion, $\tau_{\text{acc}} = M/\dot{M}$, relative to that of Kelvin-Helmholz (KH) contraction, τ_{KH} , as shown in Figure 4.

(1) During the stage with the filled square in Figures 3 and 4, $\tau_{\text{acc}} \sim \tau_{\text{KH}}$, so that the radiative luminosity (L) is supplied by the gravitational energy release due to mass accretion. The star does not contract, i.e., the radius stays almost constant. (2) During the stage between the filled square and the star mark in Figures 3 and 4, the accretion timescale gets longer than the radiative energy loss, i.e., $\tau_{\text{acc}} > \tau_{\text{KH}}$. Thus the KH contraction releases the gravitational energy at enough rates to supply the radiative luminosity. Consequently the star contracts as seen as the decrease in the radius (Figure 3). During these stages our results reproduce a similar trend as found by Yoshida et al. (2006).

3.2. Main-Sequence Phase

In the stellar interior the temperature rises during the KH contraction. Because of the absence of primordial CNO elements, hydrogen burning takes

place through the pp -chain, which does not produce high enough nuclear energy generation rate L_n to stop the KH contraction (i.e., $L_n < L$). Eventually, the central temperature (T_c) exceeds $\sim 10^8$ K and the 3α reaction starts to produce ^{12}C . When the mass fraction of ^{12}C reaches $X(^{12}\text{C}) \sim 10^{-10}$ at $T_c \sim 10^8$ K, the CNO cycle starts to produce high enough L_n . The star then settles into the main-sequence phase with $L \sim L_n$. This is approximately the turning point in the stellar radius after the KH contraction (see Figure 3). The starting point of the main-sequence is indicated by the filled star marks in Figure 3.

For model Y-1, it takes $\sim 10^5$ yr for the star to reach the main-sequence, and at this stage the stellar mass reaches several $\times 10 - 100M_\odot$, already in massive star range. Model YII is the only case in which accretion stops during the KH contraction phase. For all other models, accretion continues after reaching the main-sequence. Pop III massive stars with $M \gtrsim 10M_\odot$ keep the central temperature as high as $T_c \sim 1.0 - 1.5 \times 10^8$ K through the main-sequence. The stellar luminosity is of the order of $\sim 10^6 - 10^7L_\odot$. The main source of nuclear energy generation is the CNO cycle, and such high temperature is necessary to supply high enough nuclear luminosity to keep $L \sim L_n$ with $X(\text{CNO}) \sim 10^{-10} - 10^{-8}$. For ‘M-series’, accretion stops during the main-sequence. For YII model, accretion stops before the main-sequence. After the accretion stops, the star evolves vertically (i.e., $M = \text{constant}$) in Figure 3. For ‘Y-series’, mass accretion continues throughout the evolution. The accretion rate has decreased to $\tau_{\text{acc}} \gg \tau_{\text{KH}}$, so that the star changes its structure to adjust to the main-sequence structure of the increased M . Thus the star evolves approximately along the main-sequence line in Figure 3 where the stellar radius increases with mass ($R \propto M^{0.75}$). The main-sequence phase is the longest in the stellar life, and thus the final mass is mostly determined by how much mass accretes through the main sequence. The filled circles in Figure 3 show the end of the main sequence (hydrogen exhaustion at the center). The star grows to be very-massive. The details are summarized in section 3.3. After central hydrogen burning, central helium burning follows. The star expands and the stellar radius becomes more than 10 times larger at the end of helium burning than that on the main sequence.

Figure 5 shows the evolution of each model on the HR diagram. These figures correspond to Figure 8 in Omukai & Palla (2003). During the early mass accretion phase, the stellar radius gets larger and the surface effective temperature decreases to as low as $\sim 6000\text{K}$. The H^- bound-free opacity is the main source of opacity around this temperature. After this phase, the star undergoes the KH contraction to decrease its radius. The effective temperature gets higher to reach $\sim 10^5$ K. The main opacity source changes from H^- bound-free absorption to electron scattering at such high temperatures. The star reaches the main-sequence and evolves on the HR diagram along the main-sequence line with increasing mass. As hydrogen is consumed, the star leaves the main-sequence to decrease its effective temperature. At the end of hydrogen burning, the stellar mass reaches near its final mass.

Figure 6 shows the evolutionary changes in stellar luminosity with increasing mass. For comparison, the main-sequence points of several stars with no mass accretion are also shown. After reaching the main-sequence, the stars evolve along the main-sequence lines of corresponding stars with no mass accretion. Figure 7 shows the evolutionary tracks of the central density (ρ_c) and central temperature at later phases through carbon, neon, oxygen, and silicon burning for four models. For comparison, we also show those of the $25M_\odot$ star (Umeda & Nomoto 2002) and the $1000M_\odot$ star (Ohkubo et al. 2006) with no mass accretion. Generally, more massive stars have higher entropies (lower densities) at the same temperatures. For the model with mass accretion, the central entropy is determined when the stellar mass is small, and remains low because of the small $\tau_{\text{acc}}/\tau_{\text{KH}}$ even when the stellar mass becomes much larger. After H is ignited, the central density-temperature path moves toward higher entropy, while the central temperature is kept at $T_c \sim 1 \times 10^8$ K.

3.3. Stellar Lifetime and the Final Mass

After helium burning (at $\log T_c$ (K) ~ 8.5), the star with mass accretion evolves almost parallel to stars with no mass accretion in the (ρ_c, T_c) diagram. This is because the evolutionary timescale is $\lesssim 10^4$ yr from central helium exhaustion to core-collapse or explosion, and $\lesssim 1$ yr after T_c reaches

10^9K which is much shorter than the accretion timescale ($\tau_{\text{acc}} = M/\dot{M}$). Thus, the star evolves with negligible effects of mass accretion, and the stellar mass can be regarded as constant, reaching its final value $M = M_f$.

The final mass, M_f , is determined by the stellar lifetime and mass accretion rate. In Table 2 these results are summarized. The final mass for ‘Y-series’ is very large. This is primarily due to the long lifetime of the star. Ohkubo et al. (2006) calculated the evolution of CVMS models with $M = 500M_\odot$ and $1000M_\odot$ with no accretion. The lifetime of CVMS ($M \gtrsim 300M_\odot$) without accretion is $\sim 2 \times 10^6$ yr, which does not sensitively depend on the mass because the $M - L$ relation is close to $L \propto M$. On the other hand, our models with mass accretion have longer lifetime, $\gtrsim 3 \times 10^6$ yr, even if the final mass exceeds $300M_\odot$. Stars with mass accretion evolve through the lower mass phase. This makes stellar lifetimes longer. On the other hand, for model M-1, the lifetime is as short as 2.2×10^6 yr, much shorter than models Y-4 and Y-5, even though the final mass is in the same range. For model M-1, accretion stops after 1×10^5 yr, just after hydrogen burning starts. At this stage the star has already reached the VMS range so that the luminosity (and thus hydrogen consumption speed) is very high.

3.4. Final Phases of Evolution and Final Fate

For models Y-1, 2, 3, 4, and M-1, M_f exceeds $300M_\odot$ so that they end their life with iron core-collapse. Model Y-5 has $M_f = 275M_\odot$ and ends its life as a PISN. For models YII, M-2, and M-3 the final mass is too small to become a PISN. These stars collapse to form a black hole. Whether a star explodes as a PISN or causes iron core collapse is decisively important for galactic chemical evolution and the origin of elements. Main features of the final phases of evolution of these models are summarized below and more details will be published elsewhere.

When central helium is exhausted, the CO core contraction accelerates. Figure 8 shows the time scale of the increase in the central temperature ($\tau_T \equiv dt/d\ln T_c$) for models Y-1 ($M_f = 915M_\odot$) and YII ($M_f = 40M_\odot$). From $\log T_c$ (K) = 8.6 to 9.2, τ_T decreases drastically from $\sim 10^5$ yr to

$\sim 10^{-4}$ yr for model Y-1. At $\log T_c$ (K) = 9.2, model Y-1 is dynamically collapsing with such short τ_T , while less massive model YII still undergoes quasi-static evolution with $\tau_T = 10^0$ yr. For all cases, the core evolution accelerates, being decoupled from the envelope.

3.4.1. Stars with $M_f \simeq 140 - 300M_\odot$

Model Y-5 ends as a PISN because it enters the pair-instability region at $\log T_c$ (K) ~ 9 as seen in Figure 7, where the dynamically unstable region for the core with the adiabatic exponent $\gamma < 4/3$ is indicated. The central region collapses, which induces thermonuclear runaway of oxygen and silicon burning due to the rapid temperature increase. The thermal pressure generated by the runaway nuclear burning stops the core contraction and expands the star (Rakavy et al. 1967; Ober et al. 1983; Bond et al. 1984; Glatzel et al. 1985; Woosley 1986). This appears as the turning point of the evolutionary tracks in Figure 7. The calculation is stopped when the total energy of the star becomes positive, which leads to the total disruption of the star.

3.4.2. Stars with $M_f \gtrsim 300M_\odot$

Models Y-1, 2, 3, and 4 enter the pair-instability region in Figure 7. However, they do not explode as PISNe but undergo core-collapse to become black holes. These very massive stars have such large gravitational binding energy that the nuclear energy release can not exceed this binding energy. More details of the evolutionary processes of model Y-1 are as follows.

Figure 9 shows the chemical evolution in the interior of model Y-1 ($M_f = 915M_\odot$). Helium is exhausted in the core around $t_{\text{collapse}} - t \sim 10^4$ yr. When carbon is ignited at $t_{\text{collapse}} - t \sim 10^{-4}$ yr, the central region enters the pair instability region.

During collapse ($t_{\text{collapse}} - t \lesssim 10^{-6}$ yr), the silicon layer and iron core rapidly grow in mass. This is because in the intermediate region ($M_r \sim 100 - 200M_\odot$) oxygen and silicon burn explosively with the time scale of core collapse. Figure 10 shows the abundance distribution for model Y-1 at $\log T_c$ (K) = 10.3 and $\log \rho_c$ (g cm $^{-3}$) = 10.0. One can see that the mass of the iron core of CVMS is large ($\sim 20 - 25\%$ of the total stellar mass), much

larger than ordinary massive stars such as $\sim 10\%$ in the $25M_{\odot}$ star. This result agrees with that of 500 and $1000M_{\odot}$ stars in Ohkubo et al. (2006).

3.4.3. Stars with $M_f \lesssim 140M_{\odot}$

The final mass of model YII ($M_f = 40M_{\odot}$) is in the range of ordinary massive stars ($\lesssim 60M_{\odot}$), and so the evolutionary track is similar to that of $25M_{\odot}$ in the top panel of Figure 7. It ends with core-collapse and forms a black hole.

Model M-2 ($M_f = 135M_{\odot}$) undergoes the core oscillation as seen in the (ρ_c, T_c) evolution (Figure 7, lower). The evolutionary path in the (ρ_c, T_c) plane goes through the marginally stable region against the pair-creation instability, so that the adiabatic exponent γ is close enough to induce the pulsational nuclear instability due to central oxygen and silicon burning. In stars with $80M_{\odot} \lesssim M_f \lesssim 140M_{\odot}$, slightly under the PISN mass range, such a core oscillation appears (Woosley et al. 2007; Umeda & Nomoto 2008). The nuclear energy released during the oscillation is not large enough to disrupt the whole star, so that the core contracts and central temperature and density rise again. The star finally collapses to form a black hole after several oscillations (Figure 7).

Figure 11 shows the abundance distribution for model M-2 ($M_f = 135M_{\odot}$) at $\log T_c$ (K) = 9.95, and $\log \rho_c$ (g cm^{-3}) = 9.3. Contrary to model Y-1, the iron core mass is as small as $6M_{\odot}$, being 5% of the stellar mass. One can see from Figure 7 that the evolutionary track is similar to that of the $25M_{\odot}$ star at the collapse stage. The silicon or oxygen layer does not pass through the pair instability region, unlike the VMS star. Neither the silicon or oxygen layer can follow the central iron core collapse.

4. DISCUSSION

In this paper, we have calculated the evolution of Pop III stars that undergo mass accretion. The evolution of Pop III VMS has been studied by many authors through later nuclear burning stages, collapse, and explosion (e.g., Ober et al. 1983; Bond et al. 1984; Arnett 1996; Umeda & Nomoto 2002; Heger & Woosley 2002; Ohkubo et al. 2006). These studies assumed that such stars have their large mass from their starting point of their life and the same mass has been

held through the evolution.

Previous proto-stellar calculations ended at the onset of hydrogen burning on the main-sequence. Our results show that with mass accretion the stellar mass continues to grow after the pre main-sequence phase through the main-sequence and beyond. Assuming that radiative feedback is not significant in the majority of cases, we have confirmed the conclusion of Ohkubo et al. (2006) that there is a realistic possibility for the existence of CVMSs as Pop III stars in the early universe. We find that the final mass can be very large, being in the range where a star collapses to become an IMBH ($M_f \sim 300 - 1000M_{\odot}$).

Ohkubo et al. (2006) argued that these CVMSs contribute significantly to the metal enrichment of the early universe, while preventing the over-abundance, before ending their life quickly before ordinary core-collapse supernovae and hypernovae became dominant. Ohkubo et al. (2006) also found that the abundance of ejected heavy metals in this CVMS scenario agrees well with the observed chemical abundance data from the early universe, in contrast to poor agreement of the abundance patterns of PISNe. This is because the mass ratio of each element ejected by PISNs cannot reproduce the abundance patterns of EMP stars, intergalactic medium (IGM), or intracluster matter (ICM) (Umeda & Nomoto 2002; Heger & Woosley 2002; Chieffi & Limongi 2002). Furthermore, if the majority of the first generation Pop III.1 stars are CVMSs, they will form an IMBH, not explode as a PISN. Then, the second generation (Pop III.2) stars formed under the influence of radiation from Pop III.1 stars are less massive than $\sim 100M_{\odot}$. This scenario may explain why PISN signatures are not observed in the abundance patterns.

The presence of CVMS in the early universe, if confirmed, has important implications for progenitors of IMBHs. There is an interesting suggestion that some IMBHs may have been found (Barth et al. 2005). Matsumoto et al. (2001), by using *Chandra*, reported possible identification of a $\gtrsim 700M_{\odot}$ black hole in M82 as an ultra-luminous X-ray source (ULX). More such detections have been reported as ULXs (Colbert & Mushotzky 1999; Makishima et al. 2000; Makishima 2008) and also as an object in the Galactic center (Hansen & Milosavljevic 2004).

As to the formation of SMBHs, there are several scenarios (e.g., Rees 2002, 2003). SMBHs may be formed directly from supermassive halos of dark matter (e.g., Marchant & Shapiro 1980; Bromm & Loeb 2003; Begelman et al. 2006). Madau and Rees (2001) first suggested that mini halos with black holes with mass $\sim 150M_\odot$ at redshift $z \sim 20$ will merge with each other successively to eventually form SMBHs. Ebisuzaki et al. (2001) suggested a scenario where IMBHs grow to become SMBHs by merging and swallowing of many of these objects in dense clusters. Several authors studied detectability of gravitational waves radiated by IMBH binaries at high redshifts, by observatories such as Laser Interferometer Space Antenna (LISA) (Sesana et al. 2007; Micic et al. 2007; Tanaka & Haiman 2008; Plowman et al. 2009). If CVMSs actually existed, they could be considered as natural progenitors of IMBHs. Our results offer a natural scenario for the formation of seed black holes responsible for a merger tree model. The existence of CVMS as first stars will be supported if in the future neutrinos and gravitational waves are detected from collapsing CVMSs (Suwa et al. 2009).

Our present work uses a result from a three-dimensional cosmological simulation by Yoshida et al. (2006). Volonteri et al. (2003) have shown that the merger tree scenario starting with black hole seeds of $\simeq 150M_\odot$ at $z \sim 20$ is consistent with the present day SMBH population estimated from observed quasar luminosity and mass functions. However, any relevant model must also be consistent with the presence of SMBHs massive enough (a few $\times 10^9M_\odot$) to power the bright high redshift quasars recently discovered by the Sloan Digital Sky Survey (see, e.g. a recent review by Fan 2006). Various models have been proposed to explain these high redshift powerful massive SMBHs (e.g., Volonteri & Rees 2006; Begelman et al. 2006; Tanaka & Haiman 2008; Li et al. 2007, 2008). In some of these models, the seed black holes have to be formed in hotter (virial temperature $T_{\text{vir}} \geq 10^4$ K) and more massive ($> 10^8M_\odot$) DM halos, and the BHs grow by supercritical accretion, in order to become massive enough by $z \simeq 6$. Tanaka & Haiman (2008) further extended these earlier studies and examined successful scenarios which can be constrained by both high redshift and local SMBH populations.

In some of these models (e.g., Volonteri & Rees 2006; Tanaka & Haiman 2008) the seed black holes are of the order of $100M_\odot$ formed from collapse of Pop III VMSs, while in some others the seeds are black holes of the order of $10^{4-5}M_\odot$ which are formed directly from DM halos (e.g., Begelman et al. 2006; Tanaka & Haiman 2008). Tanaka & Haiman (2008) conclude that the models with seed black holes from both models can be successful (to be consistent with both $z = 6$ and local quasar populations), but LISA observations can distinguish between them. The environment where the seed black holes are formed from more massive and hotter DM halos is quite different from that of conventional star formation models such as those of Yoshida et al. (2006). One possible interesting extension of our current work will be to adopt supercritical accretion for star formation in the environment of more massive hotter DM halos.

Tanaka & Haiman (2008) show that in a successful merger tree scenario for $z = 6$ quasar formation without supercritical accretion, if the seed black holes are $100M_\odot$ formed from Pop III stars and subsequently accrete $> \sim 60\%$ of the time, these holes must be formed rather early at $z > 30$. We note that this constraint may be eased appreciably if the seed black holes are larger instead, such as IMBHs of $\sim 1000M_\odot$ from our CVMSs. The maximum mass for seed black holes to be formed from CVMSs may still become larger if the environment of hot, massive DM halos (of $T_{\text{vir}} \geq 10^4$ K) is adopted in our future calculations.

5. CONCLUDING REMARKS

In the present study, we calculate the evolution of Pop III stars whose mass grows from the initial mass of $\sim 1M_\odot$ by accreting the surrounding gases. Our calculations cover a whole evolutionary stages from the pre-main sequence, via various nuclear burning stages, through the final core collapse or pair-creation instability phases. We calculate models with various mass accretion rates: (1) stellar mass dependent accretion rates which are derived from cosmological simulations of early structure formation (Pop III.1 stars), based on the low mass dark matter halos at redshifts $z \sim 20$, and (2) mass dependent accretion rates for zero-

metallicity but second generation (Pop III.2) stars which are affected by radiation from the first generation (Pop III.1) stars. For comparison, we also adopt mass dependent accretion rates which are affected by radiative feedback.

The final mass of Pop III.1 stars can be very large ($M \sim 1000M_{\odot}$), beyond the PISNe mass range ($140M_{\odot} - 300M_{\odot}$). Such massive stars form IMBHs, which may be the seeds for the formation of supermassive black holes. Intriguingly, it is theoretically suggested that Pop III.2 stars are less massive ($M \lesssim 40 - 60M_{\odot}$), being in the mass range of ordinary iron core-collapse stars. Such stars explode and eject heavy elements to contribute to chemical enrichment of the early universe. The stars in this mass range are favorable candidates for the elemental origin of extremely metal-poor stars in the Galactic halo. We can explain why the signature of PISNe are not seen with the scenario that Pop III.1 stars are very massive, i.e., $M \gtrsim 300M_{\odot}$ and Pop III.2 stars are less massive, i.e., $M \lesssim 40 - 60M_{\odot}$, although there is some uncertainty with radiative feedback.

The possibility of our scenario that the majority of Pop III.1 stars is CVMSs ($M \gtrsim 300M_{\odot}$) and the majority of Pop III.2 stars is ordinary massive stars ($M \lesssim 40M_{\odot}$) is attractive because it explains the chemical evolution of the early universe where the PISN mass range ($140M_{\odot} \leq M \leq 300M_{\odot}$) can be avoided. Moreover, the range we found for large mass stars offers the attractive possibility that these CVMSs are indeed progenitors of IMBHs. Although the presence of IMBHs has not been firmly established, there are various recent observational indications. If many of IMBHs indeed existed in the early universe, even if they are rare today, that will provide valuable insight to the formation of SMBHs and ultimately galaxy formation and evolution.

TO, KN, and HU would like to thank R. Hix and F.-K. Thielemann for providing us with the nuclear reaction network. ST thanks M.J. Rees for valuable suggestions and discussion. This work has been supported in part by World Premier International Research Center Initiative, MEXT, and by the Grant-in-Aid for Scientific Research of the JSPS (18104003, 18540231, 20540226, 20674003) and MEXT (17684008, 19047004, 20040004), Japan.

REFERENCES

- Abel, T., Bryan, G.L., & Norman, M.L. 2000, *ApJ*, 540, 39
- Abel, T., Bryan, G.L., & Norman, M.L. 2002, *Science*, 295, 93
- Ahn, K., & Shapiro, P. R. 2007, *MNRAS*, 375, 881
- Arnett, W. D. 1996, *Supernova and Nucleosynthesis* (Princeton: Princeton University Press)
- Baraffe, I., Heger, A., & Woosley, S. E. 2001, *ApJ*, 550, 890
- Barkat, Z., Rakavy, G., & Sack, N. 1967, *Phys. Rev. Letters*, 18, 379
- Barth, A. J., Green, J. E., & Ho, L. C. 2005, in *Growing Black Holes*, eds. A. Merloni, S. Nayakshin, & R. A. Sunyaev (Berlin: Springer), 154
- Begelman, M., Volonteri, M., & Rees, M.J. 2006, *MNRAS*, 370, 289
- Bender, R. 2005, in *Growing Black Holes*, eds. A. Merloni, S. Nayakshin, & R. A. Sunyaev (Berlin: Springer), 147
- Bond, J. R., Arnett, W. D., & Carr, B. J. 1984, *ApJ*, 280, 825
- Bromm, V., Coppi, P.S., & Larson, R.B. 1999, *ApJ*, 527, L5
- Bromm, V., & Larson, R.B. 2003, *ARA&A*, 42, 79
- Bromm, V., & Loeb, A. 2003, *ApJ*, 596, 34
- Bromm, V., & Loeb, A. 2004, *NewA*, 9, 353
- Cayrel, R., et al. 2004, *A&A*, 416, 1117
- Chieffi, A., & Limongi, M. 2002, *ApJ*, 577, 281
- Colbert, E. J. M., & Mushotzky, R. F. 1999, *ApJ*, 519, 89
- Couchman, H. M. P., & Rees, M. J. 1986, *MNRAS*, 221, 53
- Davis, M., Efstathiou, G., Frenk, C. S., & White, S. D. M. 1985, *ApJ*, 292, 371
- Ebisuzaki, T., et al. 2001, *ApJ*, 562, L19

- Fan, X. 2006, *New Astronomy Reviews*, 50, 665
- Fuller, T. M., & Couchman, H. M. P. 2000, *ApJ*, 544, 6
- Gao, L., Yoshida, N., Abel, T., Frenk, C. S., Jenkins, A., & Springel, V. 2007, *MNRAS*, 378, 449
- Glatzel, W., Fricke, K. J., & El Eid, M. F. 1985, *A&A*, 149, 413
- Haiman, Z., Thoul, A. A., & Loeb, A. 1996, *ApJ*, 464, 523
- Hansen, B., & Milosavljevic, M. 2004, *ApJ*, 593, L77
- Heger, A., & Woosley, S. E. 2002, *ApJ*, 567, 532
- Hirschi, R. 2007, *A&A*, 461, 571
- Hix, W. R. & Thielemann, F.-K. 1996, *ApJ*, 460, 869
- Ibrahim, A., Boury, A., & Noels, A. 1981, *A&A*, 103, 390
- Johnson, J. L., Greif, T. H., & Bromm, V. 2008, *MNRAS*, 388, 26
- Kudritzki, R.-P. 2000, in *The First Stars*. eds. A. Weiss, T. G. Abel, & V. Hill (Berlin: Springer), 127
- Kirshner, R. P. 2003, *Science*, 300, 1914
- Kormendy, J., & Richstone, D. 1995, *ARA&A*, 33, 581
- Li, Y. et al., 2007, *ApJ*, 665, 187
- Li, Y. et al., 2008, *ApJ*, 678, 41
- Madau, P & Rees, M. J. 2001, *ApJ*, 551, L27
- Makishima, K et al. 2000, *ApJ*, 535, 632
- Makishima, K. 2008, in *Black Holes: from Stars to Galaxies*, eds. V. Karas, et al. (Cambridge University Press), in press
- Marchant, A. B., & Shapiro, S. L. 1980, *ApJ*, 239, 685
- Marigo, P., Girardi, L., Chiosi, C., & Wood, P. 2001, *A&A*, 371, 152
- Matsuda, T., Sato, H., & Takeda, H. 1969, *Prog. Theor. Phys.*, 42, 219
- Matsumoto, H., Tsuru, T. G., Koyama, K., Awaki, K., Canizares, C. R., Kawai, N., Matsushita, S., & Kawabe, R. 2001, *ApJ*, 547, L25
- McKee, C. F., & Tan, J. C. 2008, *ApJ*, 681, 771
- Meynet, G. Ekström, S., & Maeder, A. 2006, *A&A*, 447, 623
- Micic, M., Holley-Bockelmann, K., Sigurdsson, S., & Abel, T. 2007, *MNRAS*, 380, 1533M
- Nakamura, F. & Umemura, M. 1999, *ApJ*, 515, 239
- Nakamura, F. & Umemura, M. 2002, *ApJ*, 569, 549
- Neo, S., Miyaji, S., Nomoto, K., & Sugimoto, D. 1976, *PASJ*, 29, 249
- Nomoto, K. 1982, *ApJ*, 253, 798
- Nomoto, K., & Hashimoto, M. 1988, *Phys. Rep.*, 163, 13
- Nomoto, K., Umeda, H., Maeda, K., Ohkubo, T., Deng, J., & Mazzali, P. 2003, *Nuc. Phys. A*, 718, 277
- Nomoto, K., Tominaga, N., Umeda, H., Kobayashi, K. & Maeda, K. 2006, *Nuc. Phys. A*, 777, 424
- Ober, W. W., El Eid, M. F., & Fricke, K. J. 1983, *A&A*, 119, 61
- Ohkubo, T., Umeda, H., Maeda, K., Nomoto, K., Suzuki, T., Tsuruta, S., & Rees, M. J. 2006, *ApJ*, 645, 1352
- Omukai, K. & Nishi, R. 1998, *ApJ*, 508, 141
- Omukai, K. & Palla, F. 2003, *ApJ*, 589, 677
- O'Shea, B. W., & Norman, M. L. 2006a, *ApJ*, 648, 31
- O'Shea, B. W., & Norman, M. L. 2006b, *ApJ*, 654, 66
- Ostriker, J. P. & Steinhardt, P. 2003, *Science*, 300, 1909

- Palla, F., Salpeter, E. E., & Stahler, S. W. 1983, *ApJ*, 271, 632
- Peebles, P. J. E., & Dicke, R. H. 1968, *ApJ*, 154, 891
- Plowman, J., Jacobs, D.C., Hellings, R.W, Tsuruta, S., & Larson, S.L. 2009 (Philadelphia: IOP Publishing), in preparation
- Rakavy, G., Shaviv, G., & Zinamon, Z. 1967, *ApJ*, 150, 131
- Rakavy, G., & Shaviv, G. 1968, *Astrophys. Space Sci*, 1, 429
- Rees, M. J. 2002, in *Lighthouses of the Universe: Most Luminous Celestial Objects and Their Use for Cosmology*, eds. M. Gilfanov, R. Sunyaev, & E. Churazov (Berlin: Springer), 345
- Rees, M. J. 2003, in *The Future of Theoretical Physics and Cosmology*, eds. G. W. Gibbons, E. P. S. Shellard, & S. J. Rankin, (Berlin: Springer), 217
- Sanchez, N., et al. 2006, *MNRAS*, 366, 189
- Sesana, A., Volonteri, M., & Haardt, F. 2007, *MNRAS*, 337, 1711S
- Spergel, V., et al. 2007, *ApJS*, 170, 377
- Stahler, S. W., Palla, F., & Salpeter, E. E. 1986, *ApJ*, 302, 590
- Suwa, Y., Takiwaki, T., Kotake, K., & Sato, K. 2009, *ApJ*, in press
- Tan, J. C., & McKee, C. F. 2004, *ApJ*, 603, 383
- Tanaka, T. & Haiman, Z 2008, arXiv: astro-ph/0807.4702
- Tegmark, M., Silk, J., Rees, M. J., Blanchard, A., Abel, T., & Palla, F. 1997, *ApJ*, 474, 1
- Umeda, H., Nomoto, K., & Nakamura, T. 1999, in *The First Stars*, eds. A. Weiss et al. (Berlin: Springer), 150 (astro-ph/9912248)
- Umeda, H. & Nomoto, K. 2002, *ApJ*, 565, 385
- Umeda, H. & Nomoto, K. 2005, *ApJ*, 619, 427
- Umeda, H. & Nomoto, K. 2008, *ApJ*, 673, 1014
- Volonteri, M., Madau, P., & Haardt, F. 2003, *ApJ*, 593, 661
- Volonteri, M. & Rees, M.J. 2006, *ApJ*, 650, 669
- Yoshida, N., Abel, T., Hernquist, L., & Sugiyama, N. 2003, *ApJ*, 592, 645
- Yoshida, N., Oh, S. P., Kitayama, T., & Hernquist, L. 2007, *ApJ*, 663, 687
- Yoshida, N., Omukai, K., Hernquist, L., & Abel, T. 2006, *ApJ*, 652, 6
- Yoshida, N., Omukai, K., & Hernquist, L. 2008, *Science*, 321, 669
- Woodsley, S. E. 1986, in *Nucleosynthesis and Chemical Evolution* eds. B. Hauck, A. Maeder, & G. Meynet (Switzerland:Geneva Obs.), 1
- Woodsley, S. E., Blinnikov, S., & Heger, A. 2007, *Nature*, 450, 390

TABLE 1

STELLAR EVOLUTION MODELS WITH MASS ACCRETION RATES AS A FUNCTION OF STELLAR MASS. THE MASS ACCRETION RATES dM_Y/dt AND dM_{YII}/dt ARE ILLUSTRATED IN FIGURE 1. THE MASS ACCRETION RATES dM_{Mi}/dt ARE DISPLAYED IN FIGURE 2.

Models	Mass accretion rate ($M_\odot\text{yr}^{-1}$)	
Y-1	dM_Y/dt	Equation 1
Y-2	$0.5 \times dM_Y/dt$	
Y-3	$0.33 \times dM_Y/dt$	
Y-4	$0.1 \times dM_Y/dt$	
Y-5	$0.05 \times dM_Y/dt$	
YII	dM_{YII}/dt	Equation 2
M-1	dM_{M1}/dt	Equation 3
M-2	dM_{M2}/dt	Equation 4
M-3	dM_{M3}/dt	Equation 5

TABLE 2

STELLAR LIFETIME, FINAL MASS, CO CORE SIZE, AND FINAL FATE FOR EACH MODEL.

Models	lifetime (yr)	final mass M_f (M_\odot)	CO core mass (M_\odot)	final fate
Y-1	2.3×10^6	915	370	Core-Collapse
Y-2	2.4×10^6	710	330	Core-Collapse
Y-3	2.5×10^6	610	275	Core-Collapse
Y-4	2.9×10^6	385	170	Core-Collapse
Y-5	3.1×10^6	275	123	PISN
YII	5.5×10^6	40	14	Core-Collapse
M-1	2.2×10^6	321	155	Core-Collapse
M-2	3.1×10^6	135	58	Core-Collapse
M-3	4.5×10^6	57	22	Core-Collapse

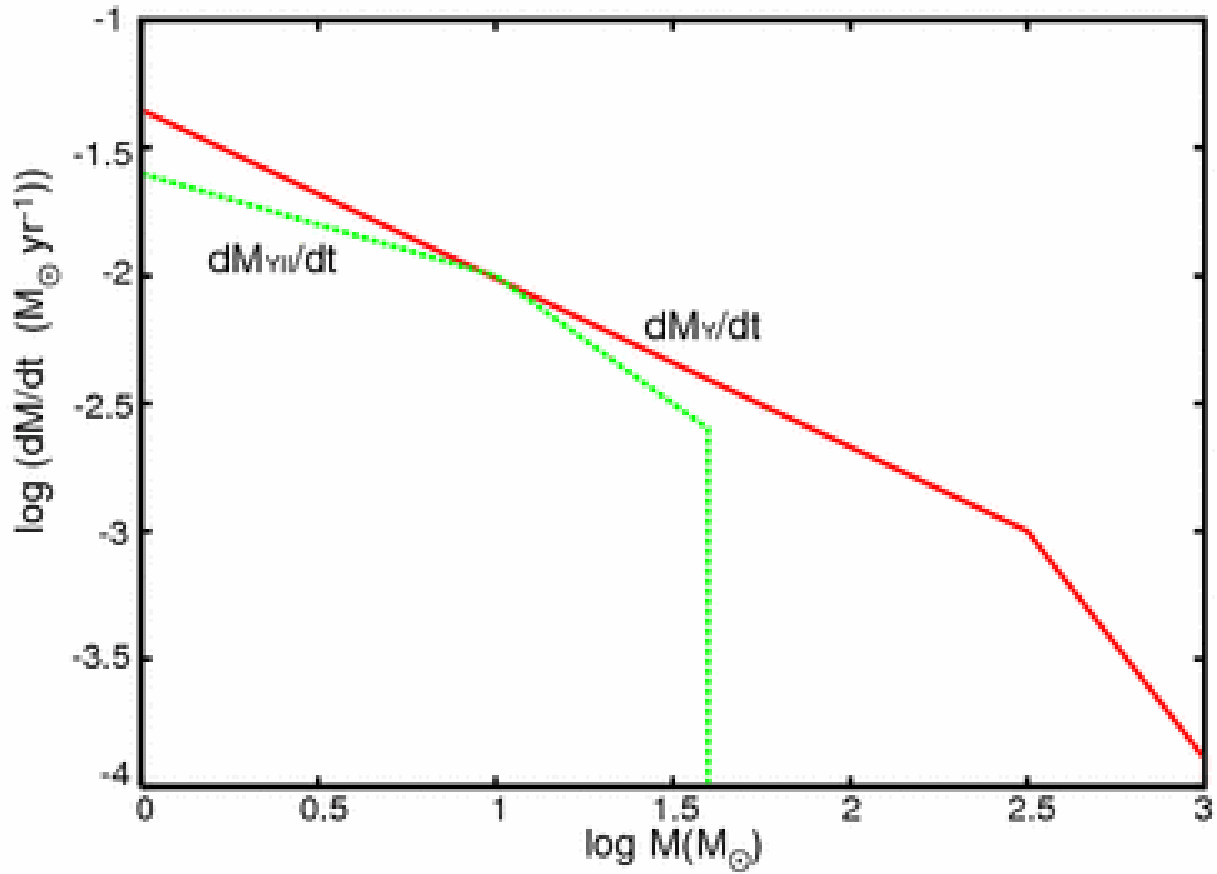


Fig. 1.— Mass accretion rates for the first generation stars (dM_Y/dt) and the second generation stars (dM_{YII}/dt) as a function of stellar mass M calculated with cosmological simulations (Yoshida et al. 2006).

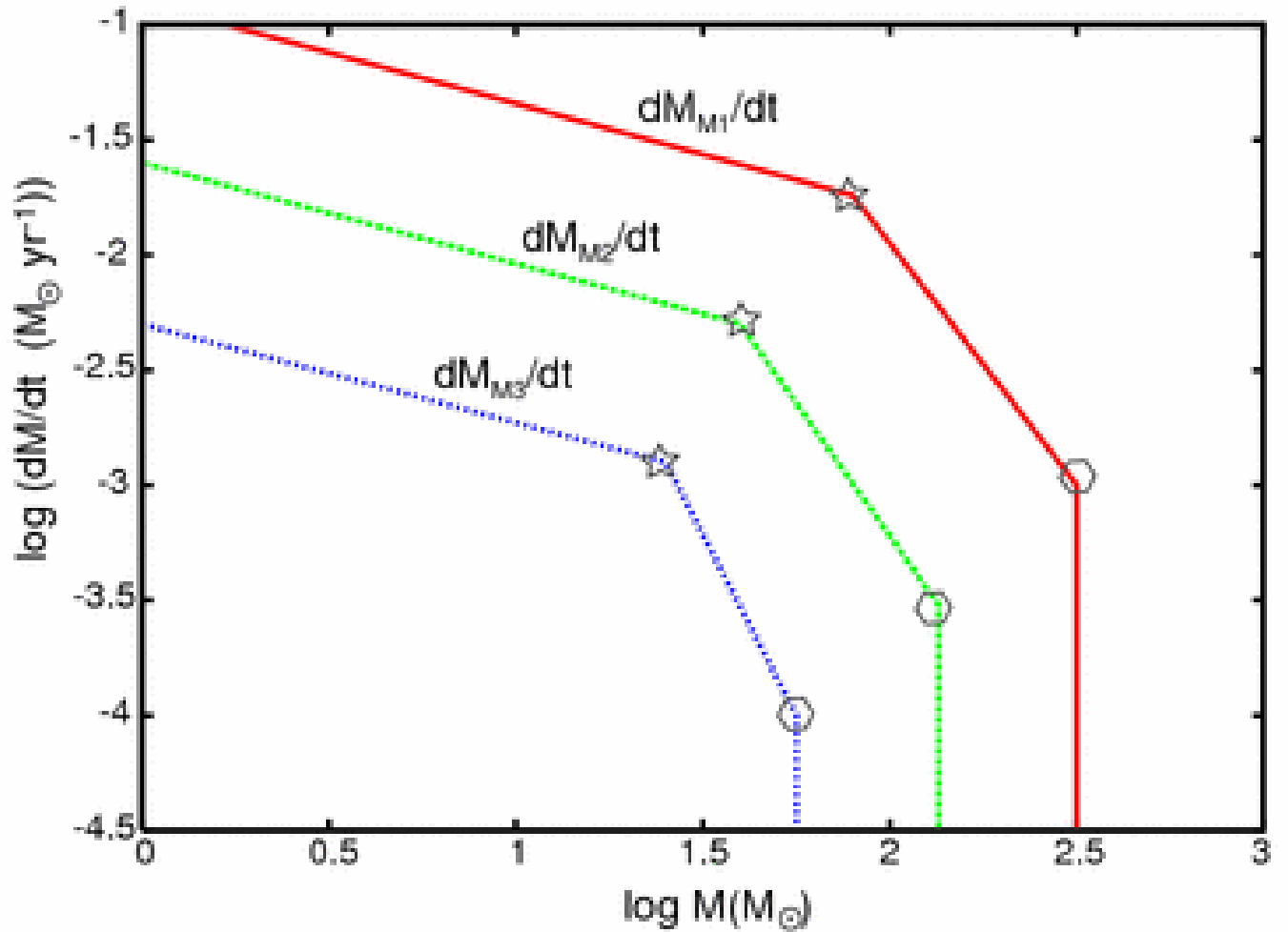


Fig. 2.— Mass accretion rates (dM_{M_i}/dt) for the first generation stars as a function of stellar mass M by McKee & Tan (2008). The open star marks show the onset of the main-sequence, after which the accretion rate drops drastically. The open hexagons show the point where the accretion completely stops.

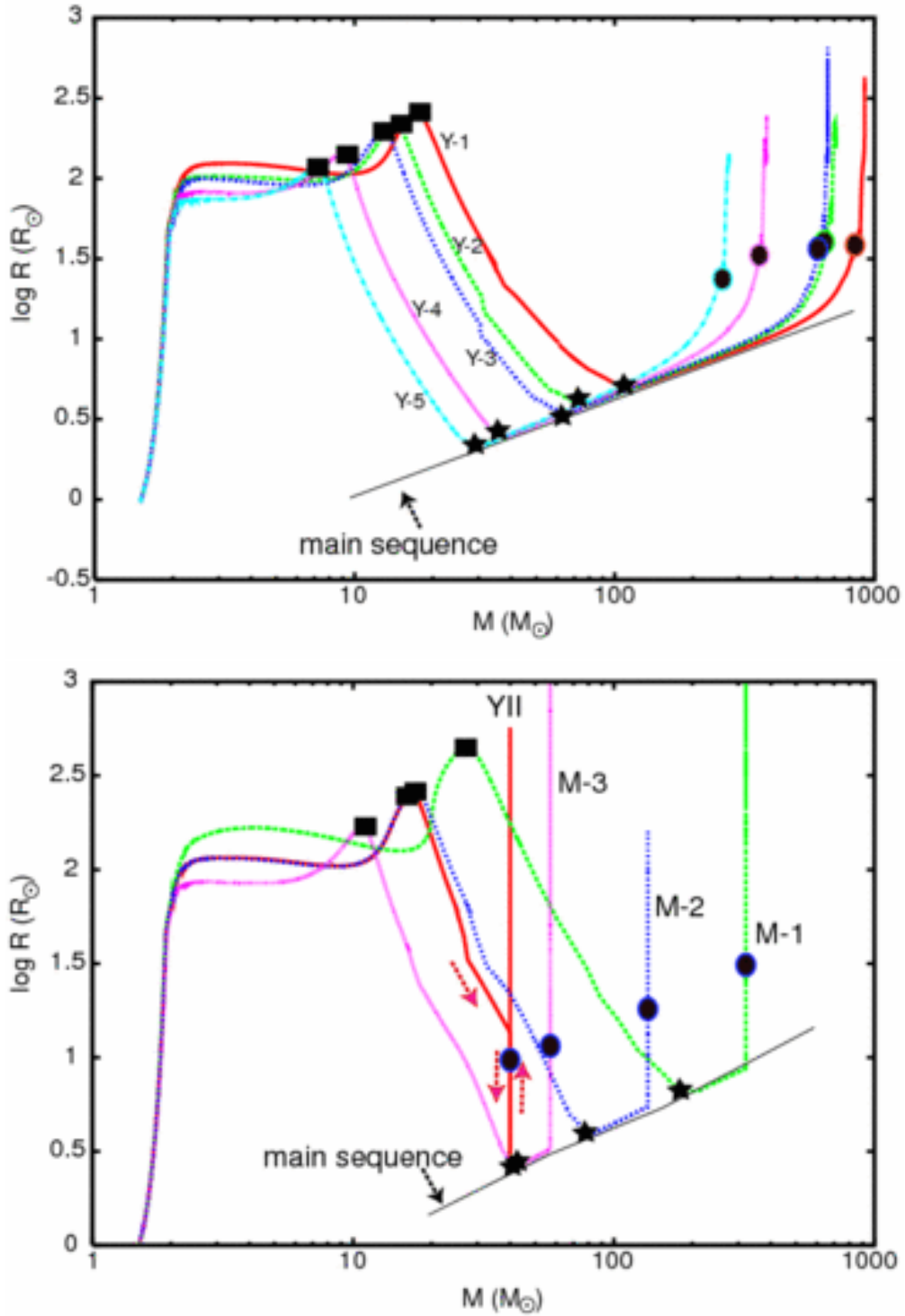


Fig. 3.— Changes in stellar radius, R , for stars evolving with increasing mass M . The top panel shows ‘Y-series’, and the bottom panel shows model YII and ‘M-series’. The arrows along the line of model YII indicates the direction of evolution. The filled squares on the lines show the beginning of Kelvin-Helmholtz (KH) contraction phase (the end of rapid accretion phase). The filled star marks are the beginning of the main sequence. The filled circles show the end of main sequence.

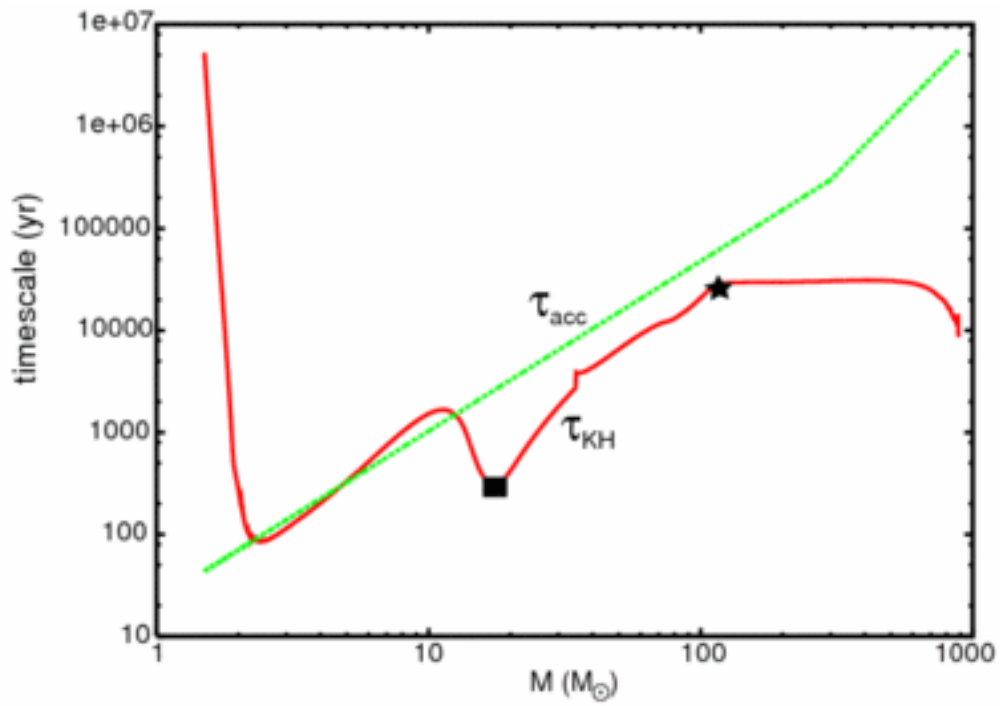


Fig. 4.— The evolutionary change in the timescales of accretion, $\tau_{\text{acc}} = M/\dot{M}$, and Kelvin-Helmholtz (KH) contraction, τ_{KH} , for model Y-1 with increasing M .

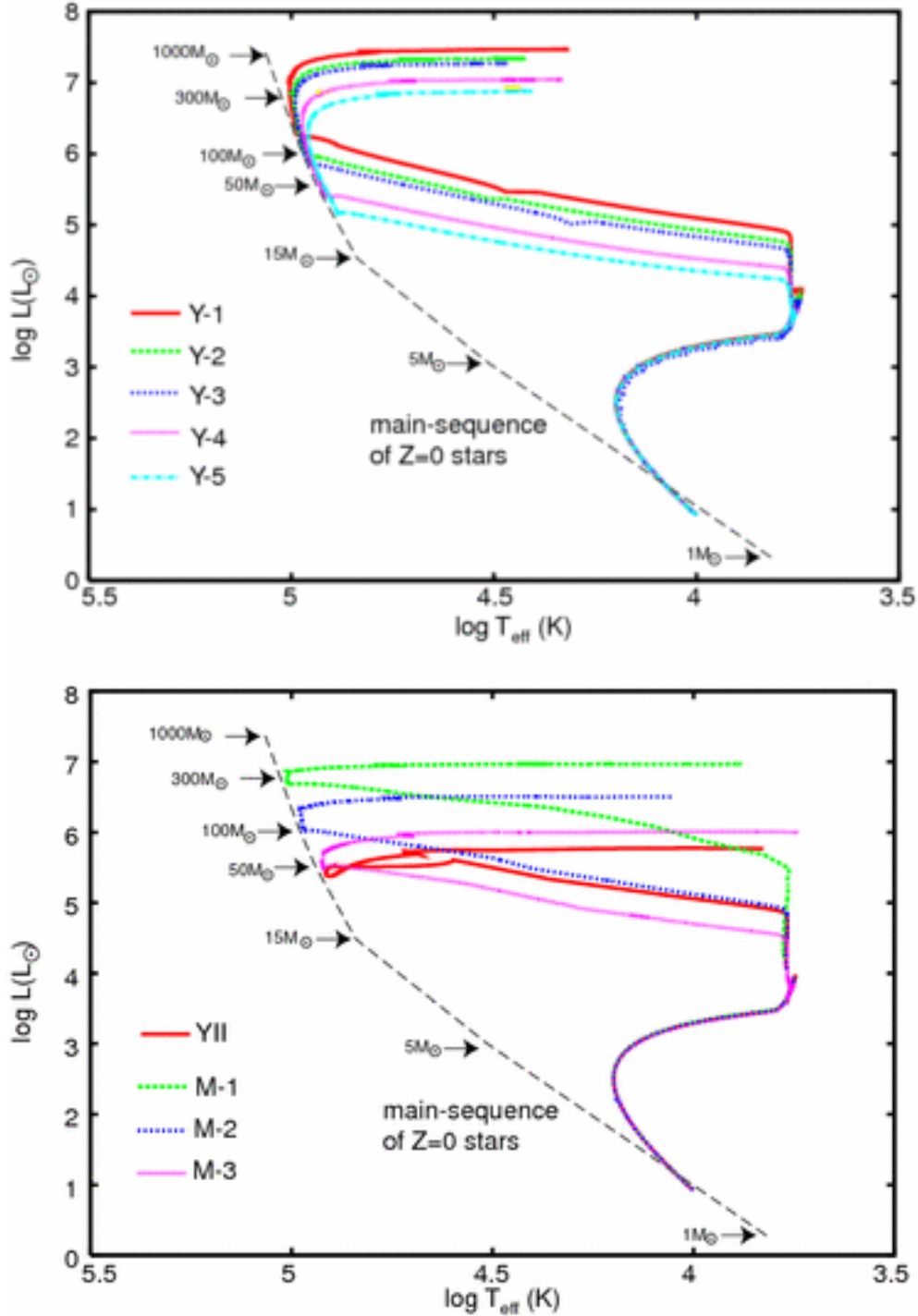


Fig. 5.— The evolution of stars with mass accretion on the HR diagram. Top panel shows ‘Y-series’, and bottom panel shows model YII and ‘M-series’. The long dashed line shows the location of main sequence stars with $Z = 0$. We adopt the location for $M \leq 100M_{\odot}$ stars from Marigo et al. (2001), and for $M \geq 100M_{\odot}$ stars from Ohkubo et al. (2006).

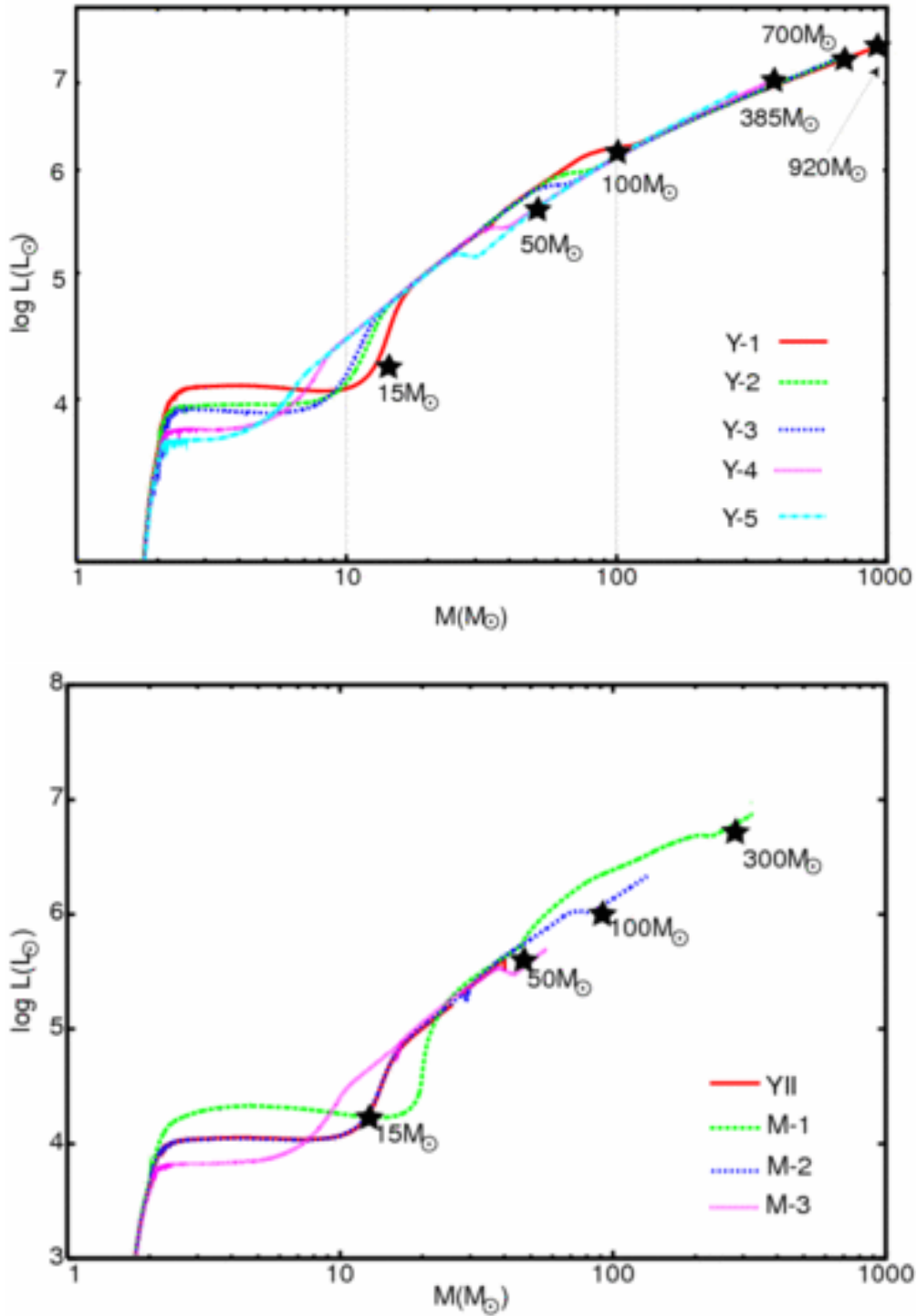


Fig. 6.— The evolutionary change in the stellar luminosity with the increasing mass, M , for ‘Y-series’ (top) and model YII and ‘M-series’ (bottom). The filled star marks indicate the main-sequence of stars without mass accretion.

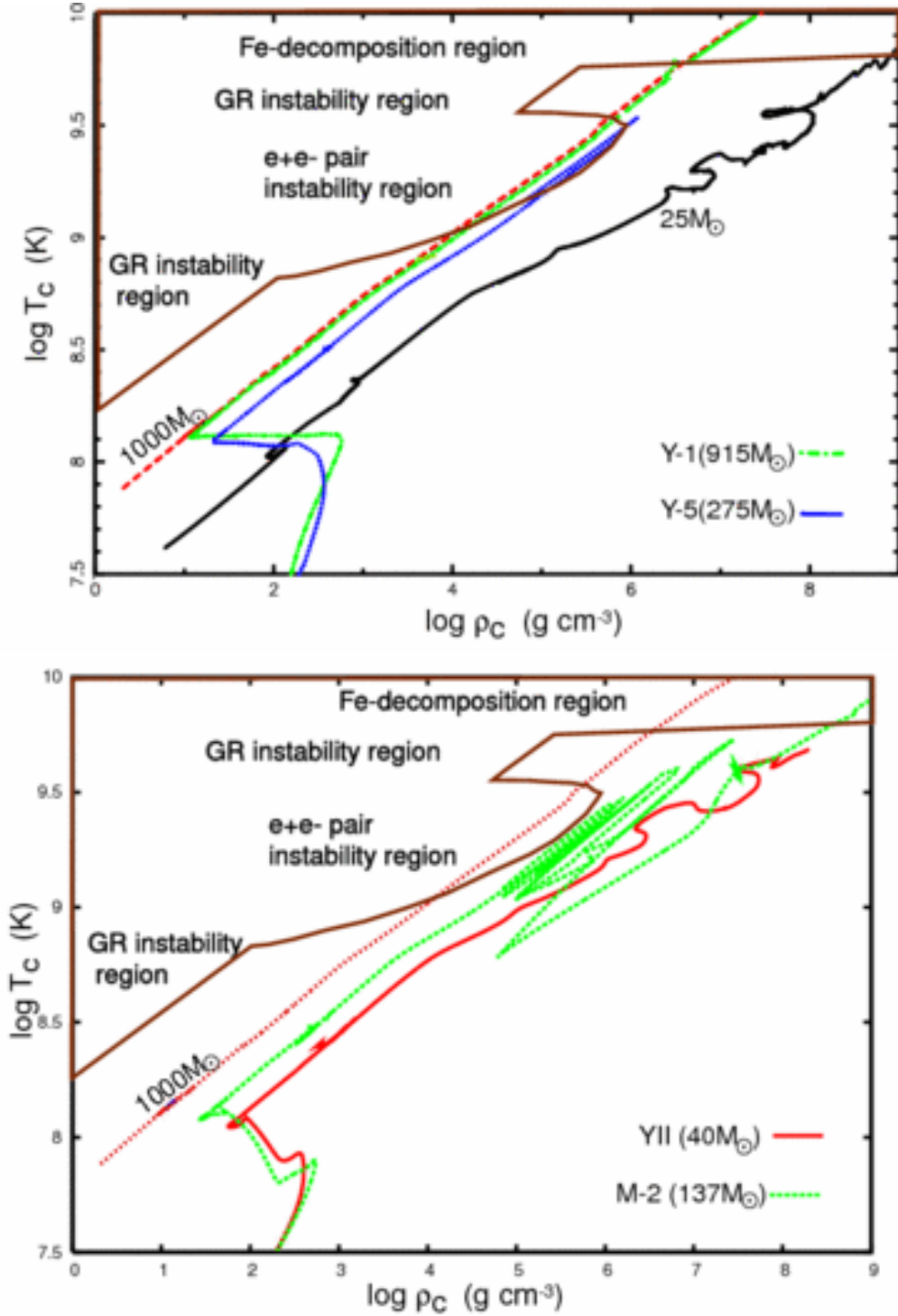


Fig. 7.— The evolutionary tracks of the central temperature (T_c) and central density (ρ_c) of models Y-1 and Y-5 (top panel) and models YII and M-2 (bottom panel). The figures in the brackets are the final mass M_f . For comparison, the tracks of $25M_\odot$ (Umeda & Nomoto 2002) and $1000M_\odot$ (Ohkubo et al. 2006) stars are also shown. The dynamically unstable regions with the adiabatic exponent $\gamma < 4/3$ are indicated.

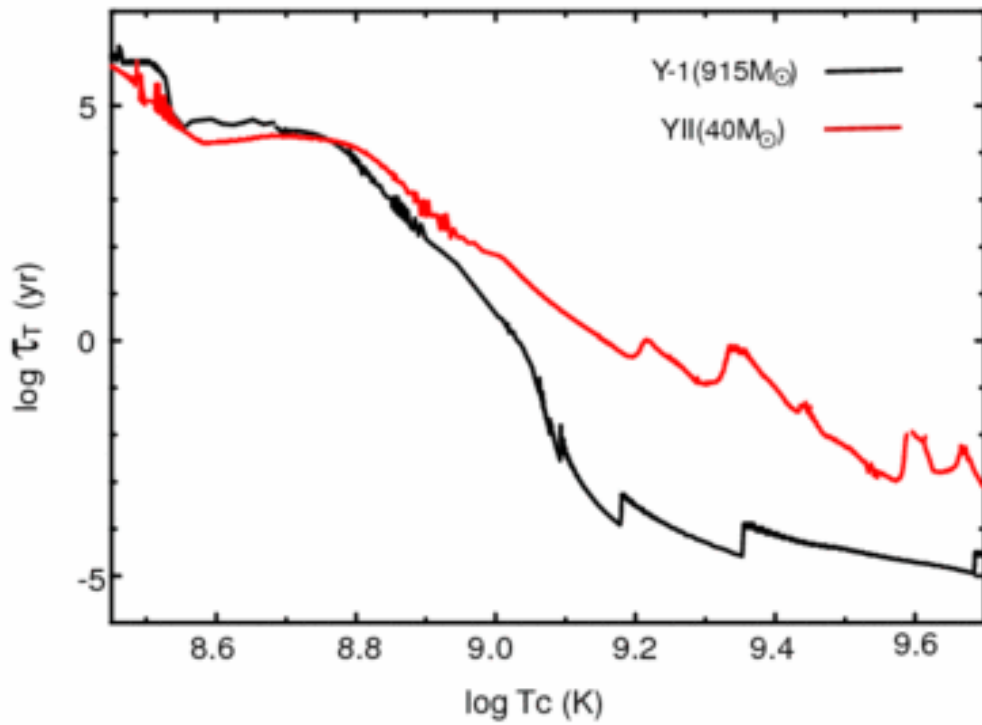


Fig. 8.— Time scale for central temperature increase, τ_T , as a function of central temperature $\log T_c$ after helium burning for models Y-1 and YII.

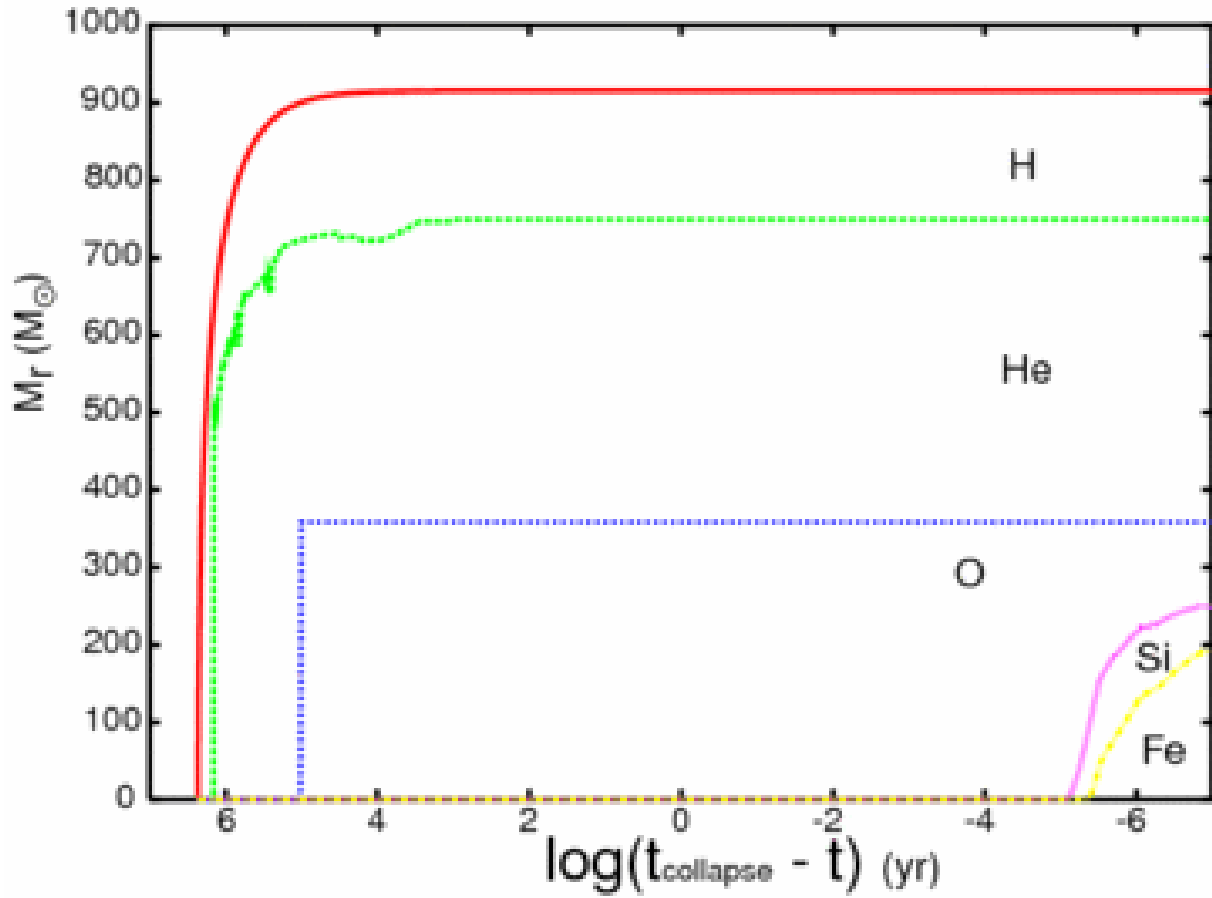


Fig. 9.— Evolution of the chemical structure as a function of time left until the core collapse for model Y-1 ($M_f = 915M_\odot$). In each layer the indicated element has the largest mass fraction.

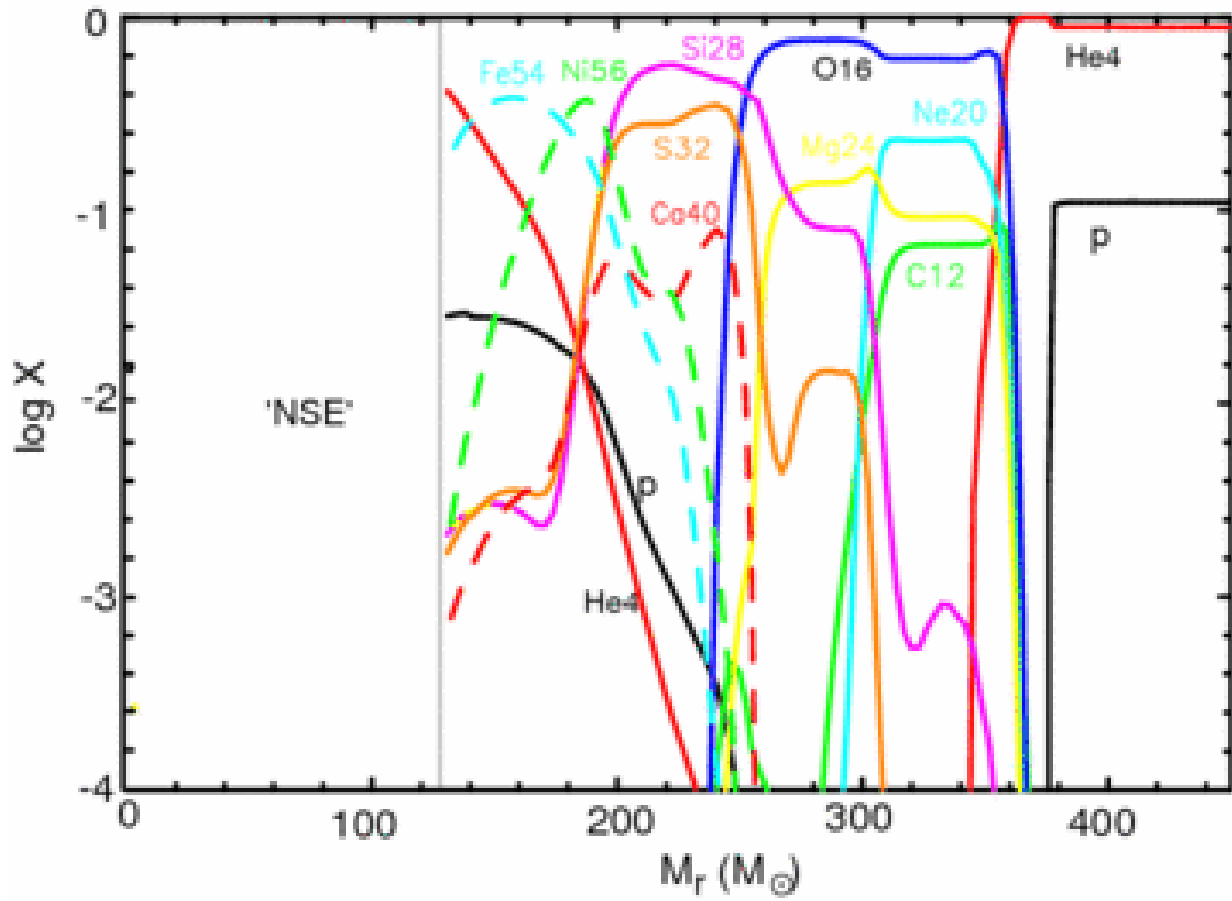


Fig. 10.— Abundance (mass fraction) distribution for model Y-1 ($M_f = 915M_\odot$) when $\log T_c$ (K) = 10.3 and $\log \rho_c$ (g cm⁻³) = 10.0.

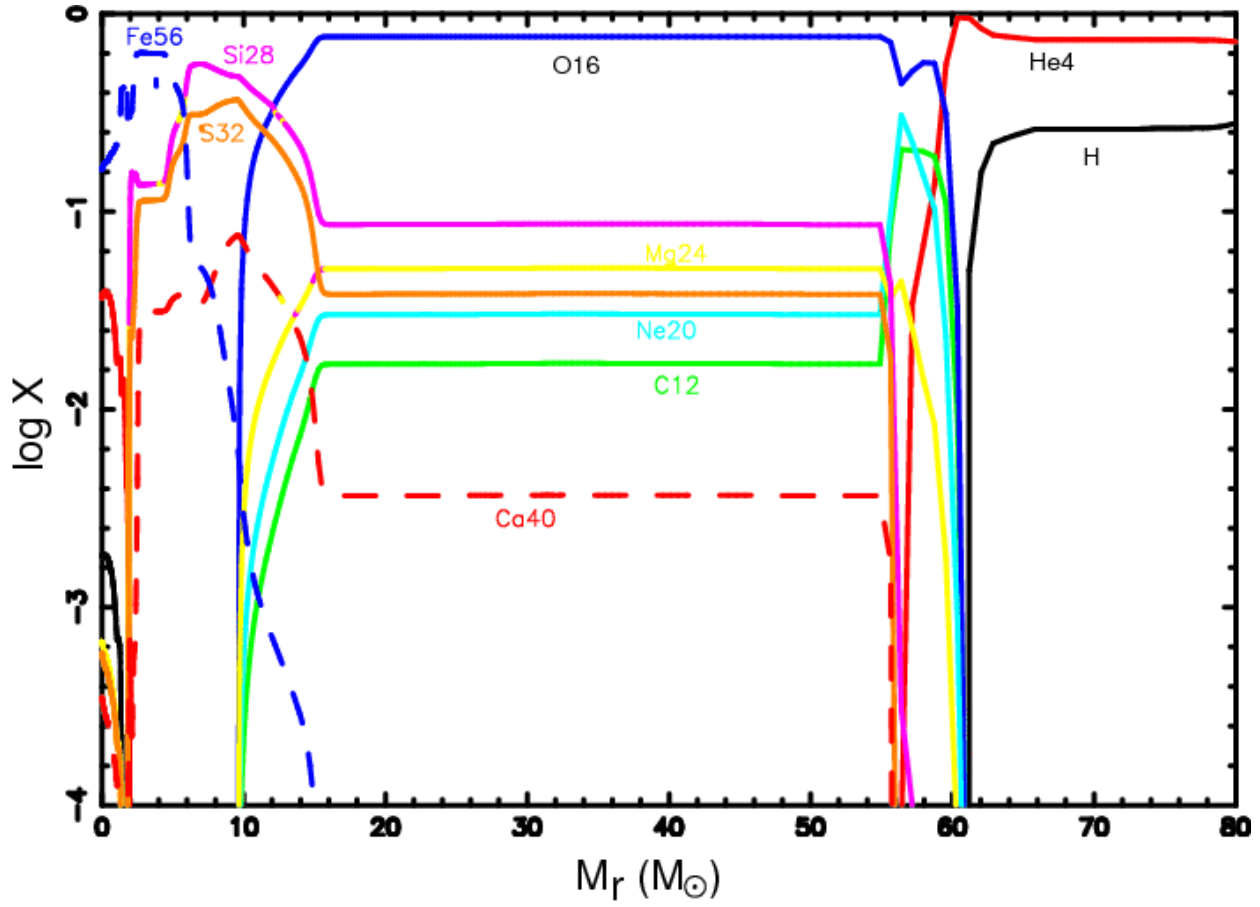


Fig. 11.— Same as Figure 10 but for model M-2 ($M_f = 135M_\odot$) when $\log T_c$ (K) = 9.95 and $\log \rho_c$ (g cm⁻³) = 9.3.